



miR-1 Induces Growth Arrest and Apoptosis in Malignant Mesothelioma

Yue Xu, PhD; Ming Zheng, PhD; Robert E. Merritt, MD; Joseph B. Shrager, MD; Heather A. Wakelee, MD; Robert A. Kratzke, MD; and Chuong D. Hoang, MD

Background: We investigated microRNA expression profiles of malignant pleural mesothelioma (MPM) specimens to identify novel microRNA that are potentially involved in the oncogenic transformation of human pleural cells.

Methods: microRNA microarray transcriptional profiling studies of 25 MPM primary tumors were performed. We used normal pleural tissue from an unmatched patient cohort as normal comparators. To confirm microarray data, we used real-time quantitative polymerase chain reaction. Representative cell lines H513 and H2052 were used in functional analyses of miR-1.

Results: In addition to several novel MPM-associated microRNAs, we observed that the expression level of miR-1 was significantly lower in tumors as compared with normal pleural specimens. Subsequently, pre-miR of miR-1 was introduced into MPM cell lines to overexpress this microRNA. Phenotypic changes of these altered cells were assayed. The cellular proliferation rate was significantly inhibited after overexpression of miR-1. Early and late apoptosis was increased markedly in miR-1-transfected cell lines. Taken together, these data suggested that overexpression of miR-1 induced apoptosis in these MPM cell lines, acting as a tumor suppressor. We confirmed our observations by assessing in the transduced MPM cells cell cycle-related, proapoptotic, and antiapoptotic genes, which all showed coordinated, significant changes characteristic of the apoptotic phenotype.

Conclusions: Further investigation and validation of our microRNA database of MPM may elucidate previously unrecognized molecular pathways and/or mechanisms by identifying novel microRNAs that are involved in malignant transformation. Our study has now found miR-1 to be one of these MPM-associated microRNAs, with potential pathogenic and therapeutic significance.

CHEST 2013; 144(5):1632–1643

Abbreviations: BDNF = brain-derived neurotrophic factor; DAPI = 4',6-diamidino-2-phenylindole; FITC = fluorescein isothiocyanate; miRNA = microRNA; MPM = malignant pleural mesothelioma; MSO = microRNA-specific oligo; PCR = polymerase chain reaction; PI = propidium iodide; qRT-PCR = quantitative real-time polymerase chain reaction; YWHAZ = tyrosine 3-monooxygenase/tryptophan 5-monooxygenase activation protein, ζ polypeptide

There is no effective cure for malignant pleural mesothelioma (MPM), which results in 3,000 deaths per year in the United States.¹ Despite aggressive treatment regimens, the median survival time remains dismal, between 4 and 18 months.² Worldwide, developing nations are increasing their asbestos imports and consumption.³ Thus, the incidence of MPM continues to rise and is likely to peak within the next 15 years in the Western hemisphere, whereas cases worldwide are predicted to rise for another 40 years.^{4,5} These data highlight the need for a more comprehensive understanding of the molecular mechanisms contributing to mesothelioma and development of innovative therapies.

Unfortunately, the molecular mechanisms controlling the malignant transformation of mesothelial cells, the originating cell type of this tumor, remain poorly defined. Aside from asbestos exposure, other factors like ionizing radiation or tumor DNA virus (simian virus-40) may act synergistically in MPM pathogenesis.⁶ Acquired genetic lesions identified in MPM include the 9p21 locus (p16INK4a, p14ARF) and the 22q11-q13.1 locus (NF2).⁷ About 20% of MPM occurrences are documented in patients without exposure to asbestos, and only 60% of MPM tumors harbor simian virus-40 DNA.⁷ Accordingly, we^{8,9} and others¹⁰ have identified multiple oncogenic pathways involved in MPM pathobiology.

Recently, another class of molecules was found that likely exert significant influence on multiple molecular pathways. microRNAs (miRNAs) are a family of short, noncoding regulatory RNA molecules expressed in a tissue-specific, developmentally regulated manner. Most miRNAs posttranscriptionally regulate the degradation or translation of target mRNAs and may function as oncogenes or tumor suppressors.^{11,12} miRNAs are frequently aberrantly expressed or mutated in cancers, and 50% of miRNA genes are located in cancer-associated genomic regions or fragile sites, suggesting a role in disease pathogenesis. The precise mechanisms of miRNAs interacting with their gene targets is complex, whereby each miRNA can control translation of tens to hundreds of different coding messengers, and a single messenger can be controlled by more than one miRNA.¹³ Despite this challenge, a growing number of reports indicate dysregulation of miRNA expression in human cancers, including MPM.

A shortcoming of previous MPM miRNA profiling studies¹⁴⁻¹⁷ is the lack of a consistent “normal” sample comparator. Although it is recognized that there are practical limitations influencing the experimental design of profiling studies, this has resulted in a myriad of potential miRNAs associated with MPM that may not have any clinical significance. Furthermore, the numbers of human MPM tissues used in prior studies are limited, so the probability of identifying key MPM-associated miRNA is much diminished. Therefore, we sought to expand on the published data by profiling a larger sampling of human primary tumors. We addressed the issue of identifying a clinically relevant normal control sample(s). We tested the validity of our profiling results by performing functional analysis on one of the most significantly altered miRNAs from our results, miRNA-1 (miR-1). miR-1 is best known as a cardiac muscle-specific miRNA transcrip-

tionally controlled by regulators of muscle differentiation¹⁸ but is increasingly observed downregulated in multiple cancers.¹⁹ Since miRNAs display both context- and tissue-specific behavior, we need to evaluate miRNA roles in diverse specimens without generalizing and assuming any miRNA will function consistently²⁰ across tumor types. Here, we show in MPM that miR-1 acts as a tumor suppressor.

MATERIALS AND METHODS

Tissues and Specimens

All available tumors, totaling 25 (epithelial = 18, biphasic = 4, sarcomatoid = 3), were obtained from the University of Minnesota Cancer Center. We included all specimens on hand, since they reflected the natural distribution of histology subtypes in this malignancy and because we were interested in identifying miRNA affecting MPM in general, as opposed to a specific subset of miRNA involved with a particular histology. Normal parietal pleura from six patients without mesothelioma or other malignancies were obtained from the Tissue Bank at Stanford Cancer Center. Approval to conduct this study was granted by the institutional review board, panel 6 of Stanford University (number 4947). These surgical specimens were collected fresh, immediately snap-frozen in liquid nitrogen, and stored at -80°C until use. All tissue specimens were verified by histopathologic studies and immunohistochemical studies (cytokeratin 5/6, 7, and 20; calretinin; E-cadherin; Ber-EP4; CD15; carcinoembryonic antigen; TTF-1; and B72.3) as containing relatively pure tumor > 80% surface area of representative slides immediately adjacent to the frozen portion of tissue used. MPM cell lines H513 (epithelial) and H2052 (sarcomatoid) were obtained from the National Cancer Institute.²¹

Chemicals and Culture Medium

RPMI-1640, fetal bovine serum, penicillin, and streptomycin were purchased from Life Technologies Corporation. Cell lines were maintained in RPMI-1640 medium supplemented with 10% fetal bovine serum and antibiotics. All cell culture wares were purchased from Corning Incorporated. Unless otherwise specified, all other chemicals were obtained from Sigma-Aldrich Co.

RNA Isolation and Microarray Processing

Total RNA enriched with miRNA was isolated using Ambion mirVana miRNA isolation kit (Life Technologies Corporation) according to the manufacturer's instructions. miRNA microarray profiling was performed at the Stanford Functional Genomics Facility (<http://sfgf.stanford.edu>). Briefly, 200 ng of total RNA extracted from tissue specimens was used as sample input for labeling and hybridization. Before labeling, RNA quality was verified on an Agilent 2100 Bioanalyzer, and only specimens with RNA integrity number > 8 were used further. A single set of Illumina, Inc Human miRNA BeadChips v2, where each BeadChip contains a total of 1,145 miRNA probes, were used for array profiling.

Briefly, the input RNA is polyadenylated and converted to cDNA by standard methods. A single miRNA-specific oligo (MSO) is used to assay each miRNA on the BeadChip. All MSOs are hybridized to the sample in parallel, and a solid-phase primer extension step further increases the specificity and reduces noise. Universal amplification of extended products only after this point avoids polymerase chain reaction (PCR)-induced detection bias. The universal PCR step creates fluorescently labeled products identifiable by their unique MSO sequence. The addressed sequence

Manuscript received November 12, 2012; revision accepted June 6, 2013.

Affiliations: From the Division of Thoracic Surgery (Drs Xu, Merritt, Shrager, and Hoang), Department of Cardiothoracic Surgery, Department of Anesthesia (Dr Zheng), and the Division of Oncology (Dr Wakelee), Department of Medicine, Stanford University School of Medicine, Stanford, CA; the Veterans Affairs Palo Alto Healthcare System (Drs Shrager and Hoang), Palo Alto, CA; and the Division of Hematology, Oncology, and Transplant (Dr Kratzke), Department of Medicine, University of Minnesota Medical School, Minneapolis, MN.

Funding/Support: Dr Hoang is supported by funds from the Mesothelioma Applied Research Foundation. The Kazan, McClain, Abrams, Fernandez, Lyons, Greenwood, Harley & Oberman Foundation, Inc provided support for the purchase of dedicated research equipment for this project.

Correspondence to: Chuong D. Hoang, MD, Stanford University School of Medicine, Falk Bldg, 300 Pasteur Dr, Stanford, CA 94305-5407; e-mail: cdhoang@stanford.edu

© 2013 American College of Chest Physicians. Reproduction of this article is prohibited without written permission from the American College of Chest Physicians. See online for more details.

DOI: 10.1378/chest.12-2770

from each MSO is used to hybridize specific miRNA products to specific locations on the bead Array substrate for readout. The Illumina iScan measures the signal intensity at each address location, which corresponds to the quantity of the respective miRNA in the original sample.

Hybridization was performed at the Stanford Functional Genomics Facility (www.microarray.org/sfgf/) according to the Illumina protocol. Axon Scanner and GenePix software (Molecular Devices, LLC) were used in scanning and postprocessing of array raw files. The microarray data are available under Gene Expression Omnibus accession number GSE40345.

MicroRNA Expression Analysis

The raw signals from the microarray were normalized by quantile-normalization available in the LIMMA package²² using R (www.r-project.org). In brief, this method can be divided into 2 steps: (1) construction of a reference distribution (which is usually unavailable in gene expression analysis context) as follows: the largest value in each microarray chip is identified and averaged to become the largest value of the reference distribution, and then the second largest value in each chip is similarly processed to become the second largest value of the reference distribution, and so on; (2) normalization of each array against the reference distribution as follows: the largest expression value in the chip is replaced by the largest value in the reference distribution, and so on. Therefore, the overall intensity distribution for all chips is made identical, but the order of the intensities for the probes in each array is different for different chips.

The empirical Bayes method²³ was applied to adjust the SD estimation of each probe on the microarray, and the false discovery rate adjustment proposed by Benjamini and Hochberg²⁴ was applied to adjust the *P* values for multiple testing. miRNA expression changes meeting our empirical, predetermined criteria (fold change > 2 and adjusted *P* value < .05) were selected for analysis. We used a selection threshold that optimizes the balance in obtaining a low false-discovery rate while identifying the highest number of significant genes.

Pre-miR-1 Transfection

Overexpression of miR-1 was accomplished by transfection of miR-1 pre-miR into MPM cell lines (H513 and H2052). Double-stranded miR-1 precursor was obtained from Life Technologies Corporation. Cells from H513 or H2052 lines were seeded into 12-well petri dishes and allowed to attach overnight. Lipofectamine RNAiMAX reagent from Life Technologies Corporation was used as a transfection control (indicated as Lipo in the figures) and a scrambled, double-stranded RNA was used as another RNA control (indicated as Mir-Neg in the figures). Alongside these controls, miRNA pre-miR (indicated as Mir-1 in the figures) was transfected into the MPM cells to overexpress miR-1. All transfection experiments were performed according to protocols from Life Technologies Corporation. RNA was harvested from the MPM cells at 48 h posttransfection to evaluate miR-1 expression. Transfection efficiency was determined by quantitative real-time PCR (qRT-PCR). At 48 h posttransfection, comparing transfected MPM cells to their parent MPM cells and the negative control cells, an average eight-fold miR-1 overexpression level was achieved. Transfection was performed in individual wells (*n* = 3). Experiments were repeated three times.

XTT Proliferation Assay

Viability and proliferation of the transfected MPM cells were assessed by Cell Proliferation Kit II (XTT assay) (Roche Diagnostics). Cells were seeded into 24-well dishes and allowed to attach overnight. At day 1, day 3, and day 6 posttransfection, cells

were labeled with the mixture of XTT labeling reagent and electron-coupling reagent. The absorbance at 490 nm was quantitated by scanning spectrophotometer, and optical density readings from cells of each group were recorded. Experiments were repeated three times, each using different batches of MPM cells. Samples (MPM cells) were prepared in triplicate for every experimental run.

Annexin V Apoptosis Assay

Fluorescein isothiocyanate (FITC) Annexin V from BD Biosciences was used to label the membrane phospholipid phosphatidylserine that occurs in apoptotic cells. At 2 days posttransfection, MPM cells were harvested and processed. FITC Annexin V (green) was added to the cell suspension. Thereafter, both 4',6-diamidino-2-phenylindole (DAPI), to stain nucleic acids, and propidium iodide (PI) (red), to stain dead cells, were added to the cell suspension. Labeled cells were analyzed by flow cytometry. The percentage of FITC- and PI-labeled cells were counted over the total DAPI-stained cells as a population of Annexin V-positive cells. These percentages from Mir-1-, Mir-Neg- and Lipo-transfected cells were calculated in each cell line investigated. Experiments were repeated three times, each using different batches of MPM cells. Samples (MPM cells) were prepared in triplicate for every experimental run.

Flow Cytometry

Flow cytometry was performed on a FACSVantage device (BD Biosciences) after appropriate setup and calibration. Details of cell staining are listed in the section describing the Annexin V assay.

DeadEnd Colorimetric Terminal Deoxynucleotidyl Transferase-Mediated dUTP-Biotin End Labeling System

A complementary method of apoptosis detection was performed using the DeadEnd Colorimetric terminal deoxynucleotidyl transferase-mediated dUTP-biotin end labeling System (Promega Corporation) on miR-1-overexpressed MPM cells. Cells were seeded on poly-L-lysine-coated glass slides inserted into culture wells. After attachment, transfection was performed, and cells were continuously cultured for 3 days. Cells were fixed in 10% buffered formalin with phosphate-buffered saline solution. All labeling procedures were carried out according to manufacturer instructions. Stained cells were detected by light microscopy, and digital images were captured at 20× resolution. Experiments were repeated three times, each using different batches of MPM cells. Samples (MPM cells) were prepared in triplicate for every experimental run.

Quantitative Real-Time PCR

Total RNA was extracted from MPM tumors and normal pleural tissues using the RNeasy Mini Kit (Qiagen) for genes and the miRNeasy Mini Kit (Qiagen) for miRNA. RNA was quantitated using NanoDrop (Thermo Fisher Scientific Inc). RNA and miRNA quality were verified on an Agilent 2100 Bioanalyzer. All samples used had RNA integrity number > 8. Reverse transcription was performed using the TaqMan Reverse Transcription Kit (Life Technologies Corporation) for genes and TaqMan miRNA Reverse Transcription Kit for miRNA. qRT-PCR was performed on the Life Technologies Corporation ViiA 7 Real-Time PCR System with appropriate assay reagents for genes and miRNA. The sequences of PCR primers for genes examined in this study are shown in Table 1. Primers were tested to determine their optimal concentrations for PCR analysis, and the resulting products were run on 2% agarose gel to confirm the appropriate size and RNA integrity. Gene expression values were normalized to the endogenous

Table 1—Probe and Primer Pair Sequences for Apoptosis and Cell Cycle-Related Genes

Gene Name	Accession Number	Primer Sequence (5' to 3')
GAPDH	NM_001256799	Forward - CCACCCATGGCAAATTCATGGCA Reverse - AACAAAGCCTGGACAAAT
P-21	NM_078467	Forward - CAGGGGACAGCAGAGGAAGA Reverse - GGGCGGCCAGGGTATGTAC
P-27	NM_004064	Forward - ATGTCAAACGTGCGAGTGTC Reverse - TCTGTAGTAGAACTCGGGCAA
P-16	NM_000077	Forward - GGGCTCTCACAAGTAGGAA Reverse - CGGAGGAGGTGCTATTAATCTC
Survivin	NM_001012270	Forward - GGCATGGGTGCCCCGAGGTT Reverse - AGAGGCCTCAATCCATGGCA
BAK	NM_001188	Forward - TGAAAAATGGCTTCGGGGCAAGGC Reverse - TCATGATTTGAAAGATCTTCGTACC
P-53	NM_001126118	Forward - CCTTCCAGAAAACTACCA Reverse - TCATAGGGCACCACCACACT
BAX	NM_138763	Forward - GGCCGGGTGTGCGCCCTTTT Reverse - CCGCTCCCGGAGGAAGTCCA
BCL-2	NM_000657	Forward - ACGGGGTGAAGTGGGGGAGG Reverse - ACACGAAGCGGTGCTTGGCA

All polymerase chain reaction experiments were repeated in triplicate.

control gene GAPDH.²⁵ miRNAs validated by PCR were obtained from Life Technologies Corporation: miR-206 (assay #000510), miR-1 (assay #002222), miR-483-5p (assay #002338), and miR-155* (assay #002287). Similarly, miRNA expression values were normalized to the endogenous control RNU44²⁶ (assay #001094). All PCR reactions were performed in triplicate. Multiple, independent experiments were conducted with high correlation (Pearson $r > 0.70$) among results.

Statistical Analysis

Means and SDs were calculated from numerical data. In the figures, bar graphs depict the mean and SD, according to that experimental run. Student t test was performed to calculate the significance. A value $P \leq .05$ was considered to be significant.

RESULTS

Study Specimens

For this study we obtained 25 specimens of MPM and six specimens of parietal pleura from patients without any cancers. The sex distribution among patients with tumors was 11 women and 14 men. Among patients with normal pleura, there were two women and four men. The age ranges were variable: 35 to 70 years old among patients with tumors and 58 to 71 years old among those with normal pleura. Table 2 indicates the details of the entire specimen cohort.

miRNA Profiling Identifies Altered miRNA and miR-1 in MPM Tissues

There were a total of 1,145 miRNAs being investigated on the BeadChip. We considered an miRNA as expressed/absent if the detection P value was $< .01$, according to Illumina recommendations. Using this criterion, the numbers of miRNAs that were present on 31 samples (25 tumors and six normal tissues) ranged

from 484 to 744. Of the 31 samples, up to 980 miRNAs were present in each sample, and 165 miRNAs were not expressed in any samples at all.

From the global microarray analysis, we performed a two-dimensional, unsupervised hierarchical clustering including all miRNAs and all specimens. The tumors clustered together based on miRNA expression profile but were distinct from the normal pleura (data not shown). After applying our criteria for significance (fold change > 2 and adjusted P value $< .05$ in tumors vs normal pleura), we found a total of 49 miRNAs overexpressed and 65 miRNAs underexpressed in MPM tumors relative to normal pleura. From our list of the 20 most differentially altered (either overexpressed or underexpressed) miRNAs, many of them have not been reported to have association with MPM by profiling as revealed in a PubMed online search. Examples of putative novel MPM-associated miRNAs include overexpressed miRs (miR-323-3p, miR-34b, and miR-514) and underexpressed miRs (miR-551b, miR-483-5p, miR-206) (Table 3). We repeated the hierarchical clustering based on 40 miRNA (top 20 overexpressed and underexpressed) and observed similar tumor and normal specimen separation patterns as with the unsupervised analysis (Fig 1A). Sarcomatoid tumors grouped to the same portion of the specimen dendrogram, indicating they were more similar, but there was miRNA profile heterogeneity among the epithelial and biphasic tumors. With the constraint of our sample size, the statistics did not support any robust correlations of miRNA profiles with clinicopathologic variables. Future meta-analyses of multiple miRNA datasets could address this issue.

We performed qRT-PCR experiments to generally validate the array profiling results. We selected four

Table 2—Patient Data

Specimen	Age, y	Sex	Histology
T1 (Epi1)	64	M	Mesothelioma, malignant
T2 (Epi2)	66	F	Mesothelioma, malignant
T3 (Epi3)	62	M	Mesothelioma, malignant
T4 (Bi1)	67	M	Mesothelioma, malignant
T5 (Epi4)	40	F	Mesothelioma, malignant
T6 (Epi5)	68	M	Mesothelioma, malignant
T7 (Epi6)	62	M	Mesothelioma, NOS
T8 (Sarc1)	68	M	Mesothelioma, malignant
T9 (Epi7)	55	F	Mesothelioma, malignant
T10 (Epi8)	45	M	Mesothelioma, NOS
T11 (Bi2)	42	M	Mesothelioma, malignant
T12 (Epi9)	41	F	Epithelioid mesothelioma, NOS
T13 (Epi10)	54	F	Mesothelioma, NOS
T14 (Epi11)	54	F	Mesothelioma, NOS
T15 (Epi12)	54	F	Mesothelioma, NOS
T16 (Epi13)	54	F	Mesothelioma, NOS
T17 (Sarc2)	67	M	Mesothelioma, malignant
T18 (Epi14)	62	M	Mesothelioma, malignant
T19 (Bi3)	35	F	Mesothelioma, malignant
T20 (Sarc3)	43	M	Mesothelioma, malignant
T21 (Epi15)	70	F	Mesothelioma, NOS
T22 (Epi16)	45	M	Mesothelioma, malignant
T23 (Epi17)	65	F	Mesothelioma, malignant
T24 (Bi4)	69	M	Mesothelioma, malignant
T25 (Epi18)	61	M	Mesothelioma, malignant
N1	71	M	Normal chest parietal pleura
N2	71	F	Normal chest parietal pleura
N3	64	M	Normal chest parietal pleura
N4	65	M	Normal chest parietal pleura
N5	62	F	Normal chest parietal pleura
N6	58	M	Normal chest parietal pleura

Bi = biphasic histology; Epi = epithelioid histology; F = female; M = male; NOS = indicates pathologic term “not otherwise specified”; Sarc = sarcomatoid histology.

miRNAs from the group of most differentially altered (Table 3) and quantitatively assessed their levels in a subset of tissues. Overall, PCR results correlated qualitatively in magnitude and direction change as determined by microarray analysis. For example, miR-206 was underexpressed 12.1-fold (tumor vs normal) in microarray and in averaged PCR expression, whereas miR-155* was overexpressed 3.8-fold in microarray and 5.2-fold in averaged PCR expression. Table 4 summarizes our PCR validations.

Our primary goal was to identify and validate biologically relevant miRNA associated with MPM. Among the significantly underexpressed miRNAs in our data, we noticed that miR-1 (6.6-fold), miR-206 (12.1-fold), and miR-133b (16.7-fold) belong to the miR-1 family and miR-133 family, all associated with regulation of mesenchymal-derived tissue.¹⁸ Similarly, these miR families may play an important role in MPM, as it is a mesenchymal-type tumor. Since we observed a low level of expression for miR-1 across many of our microarray tumor specimens (Fig 1A), and it is the most likely to be cancer associated,¹⁹ we selected it for further characterization in MPM. qRT-PCR validation

of miR-1 from the same MPM specimens showed that miR-1 was consistently underexpressed (Figs 1B, 1C).

Overexpression of miR-1 pre-miR RNA Product in MPM Cell Lines

To understand the impact of miR-1 underexpression on the mesothelioma phenotype, we selected two cell lines that represent the spectrum of MPM histology, namely epithelial (H513) and sarcomatoid (H2052). We induced overexpression of the precursor miRNA of miR-1 in these cell lines and examined the level of expression of this miRNA in the cells after transfection. Total RNA was extracted 48 h after transfection.

Table 3—Detailed List of Selected miRNA

miRNA Name	Regulation	Fold Change	Adjusted <i>P</i> Value
hsa-miR-569	DOWN	26.2	6.0E-06
hsa-miR-518e:9.1	DOWN	25.0	2.5E-10
hsa-miR-363*	DOWN	23.8	9.3E-06
hsa-miR-133b	DOWN	16.7	1.9E-04
hsa-miR-591	DOWN	15.1	5.7E-12
hsa-miR-938	DOWN	12.4	9.7E-05
hsa-miR-206	DOWN	12.1	5.7E-03
hsa-miR-1238	DOWN	9.9	1.4E-03
hsa-miR-1273	DOWN	9.6	4.1E-03
hsa-miR-144	DOWN	9.3	1.5E-04
HS_130	DOWN	8.5	9.7E-05
hsa-miR-144:9.1	DOWN	7.2	1.2E-04
solexa-7764-108	DOWN	6.8	8.1E-03
hsa-miR-486-3p	DOWN	6.7	8.7E-03
hsa-miR-1	DOWN	6.6	1.1E-02
hsa-miR-483-5p	DOWN	6.5	7.3E-03
hsa-miR-512-5p	DOWN	6.0	1.2E-03
HS_29	DOWN	5.7	5.1E-03
hsa-miR-551b	DOWN	5.3	1.3E-02
HS_35	DOWN	5.3	6.7E-03
hsa-miR-323-3p	UP	3.4	2.8E-02
hsa-miR-130b*	UP	3.5	1.9E-04
hsa-miR-221*	UP	3.7	4.1E-03
hsa-miR-409-3p	UP	3.8	9.7E-03
hsa-miR-155*	UP	3.8	1.0E-03
hsa-miR-21*	UP	3.9	1.7E-03
hsa-miR-200b	UP	4.0	4.6E-03
hsa-miR-379*	UP	4.1	1.8E-02
hsa-miR-135b	UP	4.2	1.3E-02
hsa-miR-409-5p	UP	4.3	8.6E-03
solexa-3126-285	UP	4.3	4.1E-03
hsa-miR-34b	UP	4.3	7.8E-03
hsa-miR-149	UP	4.6	4.1E-03
hsa-miR-508-3p	UP	4.6	3.0E-02
hsa-miR-200a	UP	5.3	2.1E-02
hsa-miR-509-3p	UP	5.3	2.9E-02
hsa-miR-450b-5p	UP	5.5	6.6E-04
hsa-miR-629*	UP	7.6	9.7E-05
hsa-miR-514	UP	8.4	2.4E-02
hsa-miR-212	UP	10.0	9.3E-07

We selected the top 20 most significantly altered miRNAs in our array data. The direction of regulation (up or down), the fold change (tumor samples vs normal samples), and the adjusted *P* value are all indicated. The entire microarray data are available under Gene Expression Omnibus accession number GSE40345. miRNA = microRNA.

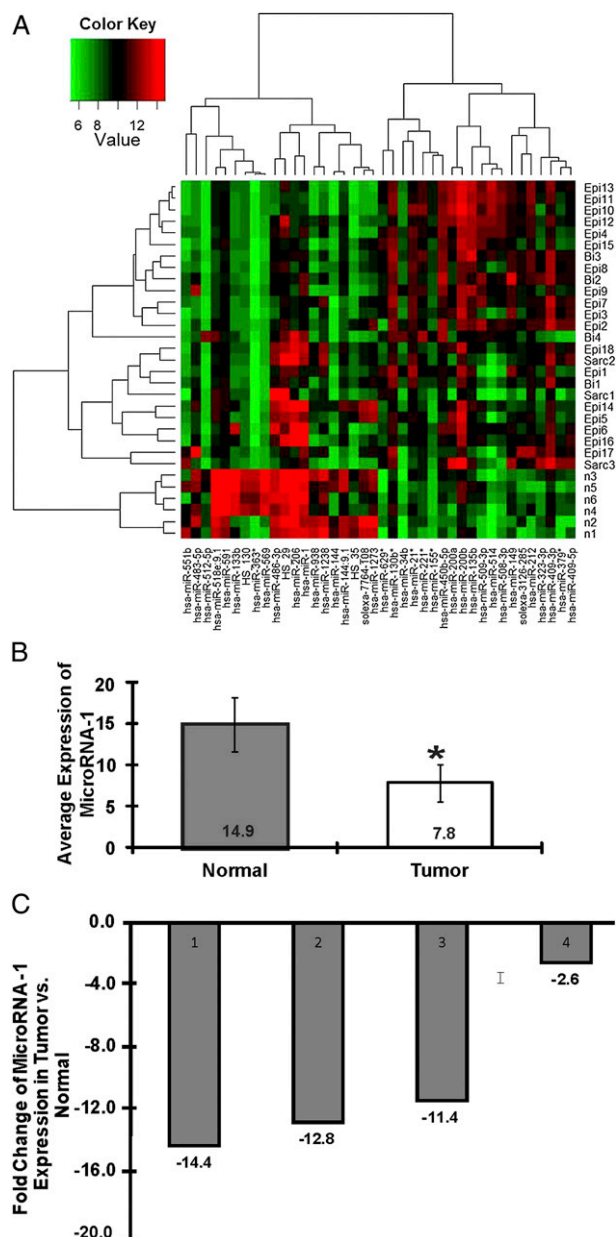


FIGURE 1. microRNA array data and expression of miR-1 in mesothelioma tumors. **A**, Unsupervised hierarchical clustering heat map for the 20 top most significantly differentially expressed microRNAs. microRNA microarray profiling was performed using Illumina Human miRNA BeadChip v2 with quantile normalization. Specific microRNAs associated with mesothelioma are shown along the horizontal axis. Specimens are along the vertical axis: 25 tumors indicated by histologic subtype (Bi = biphasic; Epi = epithelial; Sarc = sarcomatoid) and six normal tissues (n = normal pleural). Red = relative overexpression; green = relative under-expression (green). **B**, Average expression of miR-1 in primary mesothelioma tumors (n = 25) and normal pleural (n = 6) tissues. **C**, Relative fold change of miR-1 expression in representative tumors (numbered 1 to 4 along the horizontal axis) compared with normal tissues as confirmed by quantitative real-time polymerase chain reaction analysis. Specimen identity follows convention of Table 1: 1 = T8(Sarc1); 2 = T5(Epi4); 3 = T13(Epi10); 4 = T4(Bi1). *Indicates the relative change was significant ($P < .05$).

Table 4—Validation of miRNA Microarray Results by qRT-PCR

miRNA Name	T13(Epi10)	T5(Epi4)	T8(Sarc1)	T4 (Bi1)
hsa-miR-206	-16.23	-15.79	-6.49	-10.89
hsa-miR-1	-11.45	-12.85	-14.36	-2.56
hsa-miR-483-5P	-14.59	-3.68	-6.98	-5.24
hsa-miR-155*	6.29	7.89	2.98	3.45

Values represent the fold changes of the microRNA expression level in malignant pleural mesothelioma specimens as compared with pooled (n = 6) normal pleural tissue. Fold changes were calculated by the $\Delta\Delta Ct$ method. Negative indicates relative underexpression and positive indicates relative overexpression. Levels of microRNA expression were normalized to the endogenous control RNU44. PCR reactions were performed in triplicate. qRT-PCR = quantitative real-time polymerase chain reaction. See Table 2 and 3 legends for expansion of other abbreviations.

qRT-PCR was performed on miR-1 primer-specific reverse transcription products. RNU44²⁶ was used as an endogenous control for this assay. The average fold change of overexpressed miR-1 exceeded eight-fold for both cell lines we tested (Fig 2). Thus, by exogenous induction, we were able to overexpress miR-1 in MPM cell lines.

miR-1 Induces Growth Arrest in MPM Cells

We observed that cellular proliferation in miR-1-transfected MPM cell lines was markedly repressed. The XTT viability and proliferation experiments showed that cell growth in transfected cells was decreased as compared with the Lipo and Mir-Neg controls at day 1, day 3, and day 6, respectively (Fig 3). Significant ($P \leq .05$) changes in XTT dye incorporation were quantitated at day 3 and day 6, confirming our observations.

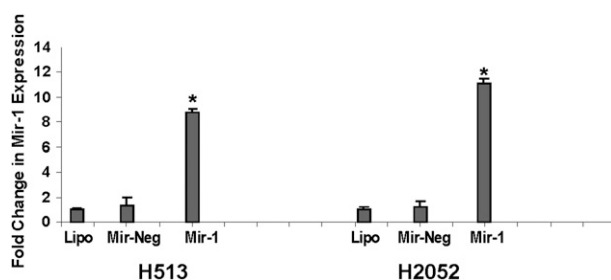


FIGURE 2. Transfection efficiency of pre-miR-1 observed in mesothelioma cell lines. Fold changes of miR-1 expression in two selected mesothelioma cell lines are shown. miR-1 pre-miR was transfected into cells using a lipofectamine-based protocol from Life Technologies Corporation. Transfection was performed in individual wells (n = 3). Experiments were repeated three times. The miR-1 expression level increased more than eightfold after induction was accomplished in both cell lines. *Indicates the relative change was significant ($P < .05$). H2052 = sarcomatoid subtype; H513 = epithelioid cell line; Lipo = lipofectamine transfection control; Mir-Neg = scrambled, double stranded RNA control; Mir-1 = microRNA pre-miR.

miR-1 Overexpression in MPM Cells Is Linked to Apoptosis

We posited that a potential explanation for the growth arrest in miR-1-transfected cells could be apoptosis. Since this process occurs in stages, we assessed both early and late stages of apoptosis with complementary assays. In separate wells, miR-1-transfected MPM cells were collected and FITC Annexin V, PI, and DAPI were used to stain preapoptotic cells, dead cells, and total cells, respectively. Flow cytometry was performed to count the different populations of cells. The percentages of FITC- and PI-positive cell populations reflected the amount of apoptosis compared with transfection control cells (Lipo) in each cell line. A significant increase ($P < .05$) in the number of apoptotic cells was observed in both MPM cell lines (H513 and H2052) after miR-1 transfection (Fig 4A). Next, we performed the DeadEnd Colorimetric terminal deoxynucleotidyl transferase-mediated dUTP-biotin end labeling assay to detect the end labels of fragmented DNA, which is characteristic of cells entering late-stage apoptosis. Concordantly, we observed a marked amount of positive staining in the miR-1-transfected MPM cells as compared with their transfection controls (Fig 4B). These two assays provide a mechanistic explanation of MPM cell growth retardation when miR-1 is introduced into cells.

Phenotype Changes in miR-1-Transfected Cells Is Associated With Alterations of Apoptotic and Cell Cycle Genes

To confirm the phenotypic changes in miR-1-transfected MPM cells, we examined genes associated with cell cycle homeostasis and apoptosis using

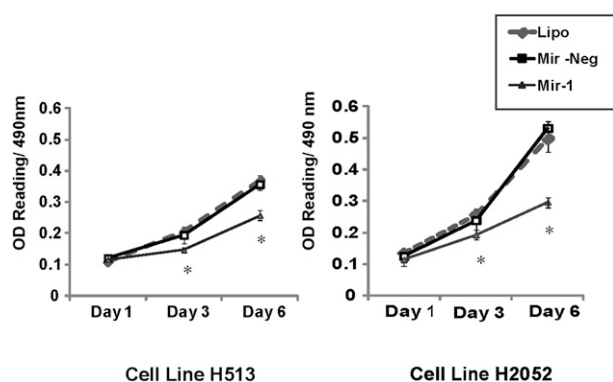


FIGURE 3. XTT growth assay. Cellular growth in cell lines H513 and H2052 after transfection of pre-miR-1. A representative experiment shows a significant decrease in growth by day 3 and day 6, indicated by * ($P < .05$). Experiments were repeated three times, each using different batches of malignant pleural mesothelioma (MPM) cells. Samples (MPM cells) were prepared in triplicate for every experimental run. OD = optical density, measured in this assay as a correlate of number of viable cells. See Figure 2 legend for expansion of other abbreviations.

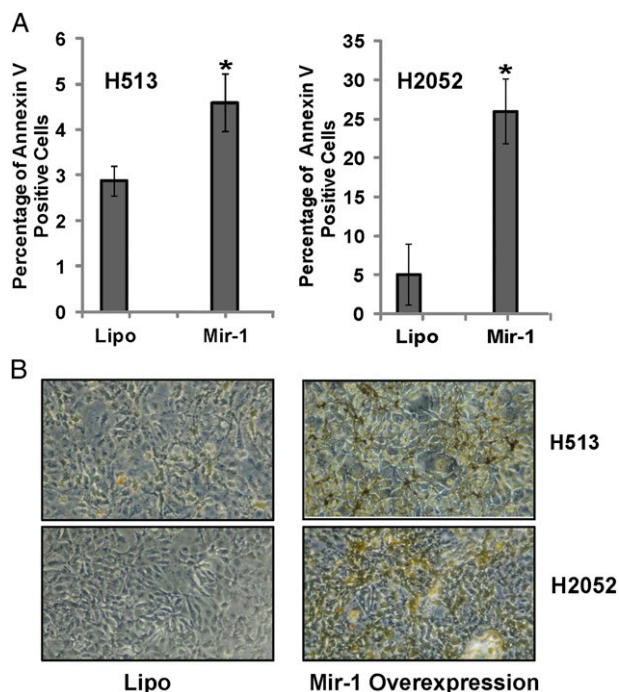


FIGURE 4. Apoptosis in cells overexpressing miR-1. A, Early apoptosis was observed by increased Annexin V-positive cells in H513 and H2052 cell lines after overexpression of miR-1. B, The terminal deoxynucleotidyl transferase-mediated dUTP-biotin end labeling assay demonstrated an increase in cell death (seen in panels on right as a yellow-brown color) after overexpression of miR-1. Experiments were repeated three times, each using different batches of MPM cells. Samples (MPM cells) were prepared in triplicate for every experimental run. Both A and B depict a representative experimental run. *Indicates the relative changes of Mir-1 overexpressed were significant ($P < .05$). See Figure 2 and 3 legends for expansion of abbreviations.

qRT-PCR. Total RNA was isolated from transfected MPM cells at 48 h posttransfection. Gene expression of p16 and p21, whose protein products affect cell cycle growth arrest, were both significantly increased ($P < .05$) in miR-1-transfected cells (Fig 5A). For cell line H2052, induction of p16 during cell cycle arrest has been described.²⁷ p53 and BAX, well known proapoptotic genes, showed significant increases in expression in these same cells as well (Fig 5B). Coordinately, the gene expression levels of the antiapoptotic genes BCL-2 and Survivin decreased (Fig 5C). Taken together, our data showed that induced overexpression of miR-1 in MPM cells resulted in appropriate changes, assuming the convention of inversely correlated expression, in genes regulating apoptosis and the cell cycle process. From a functional perspective, miR-1 behaves as a putative tumor suppressor in MPM cells.

Bioinformatics Analysis to Survey Gene Targets of miR-1

We assessed potential gene targets of miR-1 to gain further insight into potential mechanisms that explain

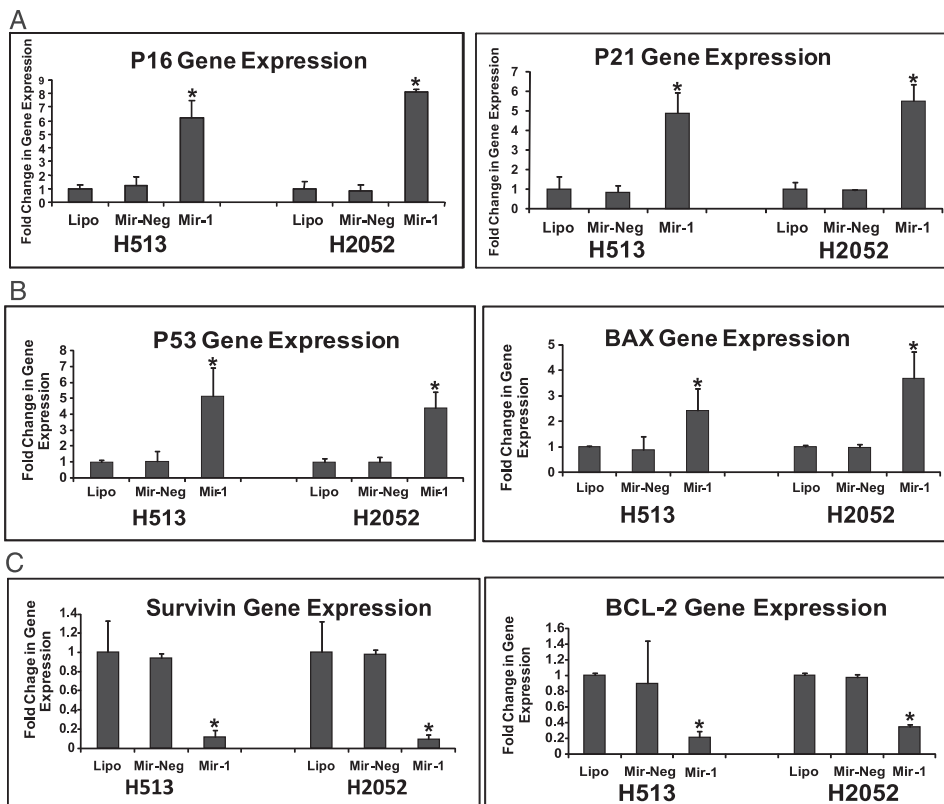


FIGURE 5. Apoptosis-related gene expression measured by quantitative real-time polymerase chain reaction (qRT-PCR). A, Cell cycle-related genes, such as p16 and p21, were increased in cell lines with miR-1 overexpression. B, Proapoptotic genes, such as P53 and BAX, were coordinately increased in the transfected cell lines. C, The antiapoptotic genes Survivin and BCL-2 were decreased in miR-1 overexpressed cells. All qRT-PCR experiments were repeated in triplicate. Fold changes were calculated by the $\Delta\Delta C_t$ method. All of the relative fold changes of Mir-1, either overexpressed or underexpressed in comparison with Lipo or Mir-Neg, were significant ($P < .05$) and indicated with *. See Figure 2 legend for expansion of abbreviations.

the tumor suppressive effect of re-expressing miR-1 in MPM cells. We used an *in silico* approach to suggest potential gene targets. Target prediction results were downloaded from three widely used prediction algorithms (as of December 2012): picTar (http://dorina.mdc-berlin.de/rbp_browser/hg18.html), miRanda (<http://www.microrna.org>, using the option: “Good mirSVR score, Conserved miRNA”), and targetScan (http://www.targetscan.org/vert_61/). Customized Perl computational scripts were used to identify the predicted targets for hsa-miR-1 in each dataset. picTar found 2,000 gene targets, miRanda found 3,017, and targetScan found 37. The union of these searches yielded a total of 29 genes that are in common across the three prediction databases. We cross-referenced each gene’s Gene Ontology (<http://geneontology.org/> as of December 2012) annotation with the term “apoptosis.” From the group of 29 genes, there were three genes associated with apoptosis: brain-derived neurotrophic factor (BDNF), DEAD box protein 3, X-chromosomal (DDX3X), and tyrosine 3-monooxygenase/tryptophan 5-monooxygenase activation pro-

tein, ζ polypeptide (YWHAZ). Please refer to Table 5 for a full description.

DISCUSSION

Since miRNAs have the ability to simultaneously regulate many target genes, thus operating as central regulators of the transcriptional repertoire,^{28,29} understanding the role of certain miRNA in MPM may reveal novel insights into the biology of this complex tumor. Identifying MPM-associated miRNAs could contribute to disease biomarker(s) discovery, molecular target discovery, mechanistic pathway analysis, and/or therapeutic development. To our knowledge, this study represents the largest of its kind aimed at finding novel mesothelioma-associated miRNA. We analyzed a total of 25 specimens of human MPM in comparison with nonmalignant pleural tissues on an approximately 1,100-miRNA microarray platform.

Prior studies of miRNA in MPM have been reported, but the body of literature is far from mature. Guled and

Table 5—Predicted Gene Targets of miR-1

Gene	Description	GO
ANKIB1	Ankyrin repeat and IBR domain containing 1	GO:0005515, GO:0008270, GO:0046872
ARID2	AT rich interactive domain 2 (ARID, RFX-like)	GO:0003676, GO:0003677, GO:0005515, GO:0005622, GO:0005634, GO:0006350, GO:0006355, GO:0008270, GO:0016568
AZIN1	Antizyme inhibitor 1	GO:0003824, GO:0004857, GO:0005515, GO:0006596, GO:0008073
BCL11A	B-cell CLL/lymphoma 11A (zinc finger protein)	GO:0003676, GO:0005509, GO:0005622, GO:0005634, GO:0005737, GO:0006350, GO:0006355, GO:0008270, GO:0030097, GO:0046872
BDNF	Brain-derived neurotrophic factor	GO:0001657, GO:0005515, GO:0006916, GO:0007406, GO:0007411, GO:0007412, GO:0007631, GO:0008038, GO:0008083, GO:0014047, GO:0016023, GO:0016358, GO:0019222, GO:0021675, GO:0042490, GO:0043524, GO:0045666, GO:0046668, GO:0048167, GO:0048839
CALM2	Calmodulin 2 (phosphorylase kinase, δ)	GO:0001539, GO:0005509, GO:0005515, GO:0005737, GO:0005886, GO:0007186, GO:0009288, GO:0031997
CLTC	Clathrin, heavy chain (Hc)	GO:0005198, GO:0005515, GO:0005739, GO:0006461, GO:0006886, GO:0008565, GO:0016020, GO:0016192, GO:0030117, GO:0030130, GO:0030132, GO:0031410
DDX3X	DEAD (Asp-Glu-Ala-Asp) box polypeptide 3, X-linked	GO:0000166, GO:0003676, GO:0003677, GO:0003723, GO:0004004, GO:0004386, GO:0005524, GO:0005634, GO:0005737, GO:0008026, GO:0016787
EFNB2	Ephrin-B2	GO:0001945, GO:0005515, GO:0005886, GO:0005887, GO:0007267, GO:0007275, GO:0007399, GO:0009653, GO:0009887, GO:0016020, GO:0030154, GO:0046875
FBXW7	F-box and WD repeat domain containing 7	GO:0001503, GO:0003700, GO:0005515, GO:0005634, GO:0005783, GO:0005794, GO:0007155, GO:0007219, GO:0016567
FNDC3A	Fibronectin type 3 domain containing 3A	GO:0001669, GO:0005829, GO:0007286, GO:0009566, GO:0012506, GO:0016337, GO:0031410, GO:0042598
FNDC3B	Fibronectin type 3 domain containing 3B	GO:0004896, GO:0016020, GO:0016021, GO:0045600
HAND2	Heart and neural crest derivatives expressed 2	GO:0001525, GO:0001701, GO:0001947, GO:0003700, GO:0005634, GO:0005667, GO:0006355, GO:0006366, GO:0006915, GO:0007275, GO:0007512, GO:0014032, GO:0030154, GO:0030528, GO:0042802, GO:0045449, GO:0045944, GO:0046982
HNRNPU	Heterogeneous nuclear ribonucleoprotein U (scaffold attachment factor A)	GO:0000166, GO:0003746, GO:0003924, GO:0005515, GO:0005525, GO:0005634, GO:0005737, GO:0005853, GO:0006414, GO:0006916, GO:0003676, GO:0003677, GO:0003723, GO:0005524, GO:0005681, GO:0006139, GO:0006397, GO:0008380, GO:0019201, GO:0030529, GO:0030530
HS3ST3B1	Heparan sulfate (glucosamine) 3-O-sulfotransferase 3B1	GO:0005794, GO:0005887, GO:0008146, GO:0008467, GO:0015015, GO:0016020, GO:0016740
JARID2	Jumonji, AT rich interactive domain 2	GO:0003755, GO:0005524, GO:0005525, GO:0005528, GO:0005622, GO:0005634, GO:0005737, GO:0006457, GO:0006463, GO:0006825, GO:0007566, GO:0016853, GO:0030674, GO:0031072, GO:0031503, GO:0035259, GO:0046661, GO:0051219, GO:0000122, GO:0001889, GO:0003677, GO:0005515, GO:0006350, GO:0007275, GO:0007417, GO:0008285, GO:0016564, GO:0048536, GO:0048538
MIPOL1	Mirror-image polydactyly 1	^a
MON2	MON2 homolog (<i>Saccharomyces cerevisiae</i>)	GO:0000139, GO:0005739, GO:0006811, GO:0006895, GO:0015986, GO:0015992, GO:0016020, GO:0016021, GO:0016469, GO:0045263, GO:0046933, GO:0046961
NCL	Nucleolin	
NR4A2	Nuclear receptor subfamily 4, group A, member 2	GO:0003677, GO:0003700, GO:0003707, GO:0003708, GO:0004879, GO:0005515, GO:0005634, GO:0006350, GO:0006355, GO:0007165, GO:0007399, GO:0008270, GO:0030182, GO:0042053, GO:0043565, GO:0045944, GO:0046872
PICALM	Phosphatidylinositol binding clathrin assembly protein	GO:0005543, GO:0005545, GO:0005794, GO:0005886, GO:0005905, GO:0006461, GO:0006898, GO:0016020, GO:0017124, GO:0030118, GO:0030136, GO:0030276, GO:0031410, GO:0045202, GO:0048268
PTMA	Prothymosin, α (gene sequence 28)	^a
RNF165	Ring finger protein 165	GO:0005515, GO:0008270, GO:0046872
TBC1D15	TBC1 domain family, member 15	GO:0005096, GO:0005097, GO:0005622, GO:0005739, GO:0032313
TMSL3	Thymosin-like 3	GO:0003779, GO:0005737, GO:0007010
VEZF1	Vascular endothelial zinc finger 1	GO:0001525, GO:0001885, GO:0003676, GO:0003677, GO:0003704, GO:0005622, GO:0005634, GO:0006350, GO:0006357, GO:0006968, GO:0008270, GO:0046872
YWHAZ	Tyrosine 3-monooxygenase/tryptophan 5-monooxygenase activation protein, ζ polypeptide	GO:0003677, GO:0003714, GO:0005634, GO:0005737, GO:0006355, GO:0008285, GO:0030528, GO:0042994, GO:0045449
ZFHX4	Zinc finger homeobox 4	GO:0003676, GO:0003700, GO:0005179, GO:0005198, GO:0005199, GO:0005576, GO:0005622, GO:0005634, GO:0006355, GO:0007155, GO:0008270, GO:0015629, GO:0043565, GO:0046872
ZNF827	^a	^a

GO = Gene Ontology. See Table 3 legend for expansion of other abbreviation.

^aNot characterized in IDConverter.

colleagues¹⁷ were among the first to globally profile miRNA in 17 MPM samples (one sarcomatoid), wherein they identified 21 differentially expressed miRNAs that seemed to recapitulate the three distinct histopathologic subtypes of MPM. Their findings were based on a comparison with a single sample of human pericardium as the normal control. The studies by Balatti and colleagues¹⁴ and Busacca and colleagues¹⁵ each reveal another set of differentially expressed miRNAs in MPM, but the specimens used for profiling ($n = 5$ or $n = 2$, respectively) in each study were all well-established MPM cell lines. The normal control samples were short-term cultures of human pleural mesothelial cells or immortalized human mesothelial cells. However, conclusions drawn from cell line data do not always corroborate in a biologically relevant manner with data from human tumors, even if the findings are validated in a larger human dataset, because of the inherent artificiality of *in vitro* systems.³⁰ Last, the only other miRNA microarray dataset related to human MPM we could identify was the study by Gee and colleagues¹⁶ that included 15 MPM samples. This study focused on identifying differential miRNA that could distinguish between MPM vs lung cancer, so the reported significant miRNAs are necessarily non-overlapping with other studies. Thus, in published reports, there are no consistent miRNAs and/or their gene targets that have been proposed to be critical to the malignant phenotype of MPM.

Our miRNA profiling approach using human tumor samples and nonmalignant pleural tissues reveals yet more differentially expressed miRNA associated with MPM. The use of primary human tumor tissues in comparison with tissue accurately representing the nonmalignant cells originating the tumor is more likely to identify clinically relevant, MPM-associated miRNA. Some of the most differentially altered miRNAs from our profiling results seem potentially interesting to MPM pathogenesis. Recently, it was demonstrated that miR-155 is involved in multiple biologic processes, such as inflammation, and is highly overexpressed in multiple solid tumors, such as in lung carcinoma, where it may play a useful role in molecular diagnostics.³¹ miR-483-5p was found to be significantly down-regulated in brain gliomas, and when it was re-expressed in cell lines, it induced G0/G1 cellular arrest via an ERK1 pathway, thereby behaving as a tumor suppressor in human gliomas.³² We note that our miRNA results showed significant overexpression of miR-155 and underexpression of miR-483-5p in MPM. miRNA exhibit tumor-specific biologic roles,²⁰ so we cannot assume the results from other tumors hold true in MPM. It is well beyond the scope of our study to know the distinct biologic functions of multiple miRNAs in MPM. Nevertheless, our results of miRNA profiling represent a valuable database for ongoing studies that

are specifically relevant to MPM and, in general, other meta-analyses involving solid tumors.

Additionally, we chose to focus on a group of under-expressed miRNAs in MPM, which are likely relevant to the malignant phenotype of MPM. Further analysis of the gene targets of this group of miRNAs could reveal new insights into the biologic mechanisms that contribute to mesothelial transformation and progression. Although dysregulation of miRNA expression in various human cancers has been reported, including chronic lymphocytic leukemia, breast carcinoma, and lung carcinoma,^{33,34} there is evidence to support the notion that miRNAs are tissue-specific and/or cancer-type specific.²⁰ Our consistent finding of miR-1 under-expression in MPM tissues suggested that this miRNA is likely associated with the malignant phenotype of MPM. Other diverse studies are consistent with our results in which there is apparent down-regulation of miR-1 in solid tumors such as hepatocellular carcinoma,³⁵ rhabdomyosarcoma,³⁶ and bladder cancer.¹⁹ Using ectopic expression of this particular miRNA in MPM cell lines representative of epithelial and sarcomatoid subtypes, we have observed cell cycle arrest and apoptosis in the MPM tumor cells and have confirmed that the underlying mechanisms responsible for this change in cell phenotype is specific to apoptosis genes, which are aberrant after miR-1 induction.

Whether miR-1 directly regulates apoptotic genes, such as BAX or BCL-2, or whether miR-1 exerts an indirect effect on the apoptotic pathway in MPM cells remains to be determined. Our preliminary *in silico* analysis suggests that miR-1 exerts its effect on apoptotic pathways indirectly via secondary mediators. All three predicted gene targets of miR-1 are not direct, canonical mediators of apoptosis but are known to participate in antiapoptotic pathways through various signaling pathways. The BDNF gene product is a growth factor that modulates Akt activity, thus comprising a BDNF-Akt-BCL-2 antiapoptotic axis.³⁷ DDX3X encodes a protein that associates with others (GASK3A/B and BIRC2) to form a complex antagonizing death receptors, providing a counterbalance to apoptotic signaling.³⁸ YWHAZ gene product is implicated in oncogenesis by antiapoptosis signaling via the JNK/p38 pathway.³⁹ Regardless of the precise molecular mechanisms leading to apoptosis, induction of miR-1 expression may be a useful therapeutic strategy to be tested in MPM native tissues.

A potential limitation of our study is the use of unmatched, nonmalignant pleura as our reference for normal. Overall, there is no consensus on what constitutes an ideal reference in a particular type of miRNA microarray experiment.⁴⁰ Certainly, using nonmalignant tissues that are the cell-of-origin of their malignant counterpart would make intuitive sense and minimize spurious identification of differentially expressed

miRNAs. The best experimental design to maximize identification of MPM-specific miRNAs would entail acquiring patient-matched normal pleura, which is not feasible given that MPM is usually a diffuse pleural disease of the entire hemithorax. Another practical constraint with miRNA profiling in general is the growing number of known unique miRNAs. According to the latest miRBase release 18, there are now about 1,898 human miRNAs (www.mirbase.org), and so not every MPM study, including ours, is able to describe the entire range of miRNA alterations in this tumor. This suggests that ongoing studies to describe miRNA associated with MPM need to be conducted, and the potential for discovery is not at all elusive.

CONCLUSION

In summary, using an experimental design based on MPM tissues and normal pleura, we identified multiple novel miRNAs significantly altered. These miRNAs warrant further investigation, as they may be clinically significant. In particular, our data demonstrate that MPM tissues express very low levels of miR-1 in a consistent manner across the entire histopathologic spectrum. We showed that introduction of miR-1 into MPM induced apoptosis. We propose that this miRNA may function as a putative tumor suppressor in MPM. Exploiting the functional role of miR-1 in MPM may translate to an effective therapeutic strategy for this complex and refractory malignancy. Additional studies are required to identify the gene targets of miR-1 in MPM and identify the molecular pathways encompassing these genes.

ACKNOWLEDGMENTS

Author contributions: Dr Hoang is guarantor of the paper, taking responsibility for the integrity of the data and accuracy of the data analysis.

Dr Xu: contributed to organizing experiments, laboratory measurements, data analysis, and manuscript writing.

Dr Zheng: contributed to laboratory measurements, data analysis, and writing of the manuscript.

Dr Merritt: contributed to study design, specimen accrual, and writing of the manuscript.

Dr Shrager: contributed to study design, specimen accrual, and writing of the manuscript.

Dr Wakelee: contributed to study design, specimen accrual, and writing of the manuscript.

Dr Kratzke: contributed to data analysis, specimen accrual, and revising of the manuscript.

Dr Hoang: contributed to conceiving the ideas, supervising the study, and writing and revising of the manuscript.

Financial/nonfinancial disclosures: The authors have reported to CHEST that no potential conflicts of interest exist with any companies/organizations whose products or services may be discussed in this article.

Role of sponsors: The sponsors had no role in the design of the study, the collection and analysis of the data, or the preparation of the manuscript.

Other contributions: We thank Sarah Howell, BS, of the University of Minnesota Tissue Procurement Facility for assistance in

handling of the tumors. We thank Steve Lee, BA, and Amanda Khuong, BS, for assistance with data management and coordinating the tissue handling at Stanford. We thank Max Bourdillon for careful assistance in manuscript preparation.

REFERENCES

1. Britton M. The epidemiology of mesothelioma. *Semin Oncol*. 2002;29(1):18-25.
2. Robinson BW, Lake RA. Advances in malignant mesothelioma. *N Engl J Med*. 2005;353(15):1591-1603.
3. Brims FJ. Asbestos—a legacy and a persistent problem. *J R Nav Med Serv*. 2009;95(1):4-11.
4. Ismail-Khan R, Robinson LA, Williams CC Jr, Garrett CR, Bepler G, Simon GR. Malignant pleural mesothelioma: a comprehensive review. *Cancer Contr*. 2006;13(4):255-263.
5. Murayama T, Takahashi K, Natori Y, Kurumatani N. Estimation of future mortality from pleural malignant mesothelioma in Japan based on an age-cohort model. *Am J Ind Med*. 2006;49(1):1-7.
6. Kaufman AJ, Pass HI. Current concepts in malignant pleural mesothelioma. *Expert Rev Anticancer Ther*. 2008;8(2):293-303.
7. Carbone M, Kratzke RA, Testa JR. The pathogenesis of mesothelioma. *Semin Oncol*. 2002;29(1):2-17.
8. Hoang CD, D'Cunha J, Kratzke MG, et al. Gene expression profiling identifies matrix metalloproteinase overexpression in malignant mesothelioma. *Chest*. 2004;125(5):1843-1852.
9. Hoang CD, Zhang X, Scott PD, et al. Selective activation of insulin receptor substrate-1 and -2 in pleural mesothelioma cells: association with distinct malignant phenotypes. *Cancer Res*. 2004;64(20):7479-7485.
10. Carbone M, Ly BH, Dodson RF, et al. Malignant mesothelioma: facts, myths, and hypotheses. *J Cell Physiol*. 2012;227(1):44-58.
11. Lu J, Getz G, Miska EA, et al. MicroRNA expression profiles classify human cancers. *Nature*. 2005;435(7043):834-838.
12. Volinia S, Calin GA, Liu CG, et al. A microRNA expression signature of human solid tumors defines cancer gene targets. *Proc Natl Acad Sci U S A*. 2006;103(7):2257-2261.
13. Peter ME. Targeting of mRNAs by multiple miRNAs: the next step. *Oncogene*. 2010;29(15):2161-2164.
14. Balatti V, Maniero S, Ferracin M, et al. MicroRNAs dysregulation in human malignant pleural mesothelioma. *J Thorac Oncol*. 2011;6(5):844-851.
15. Busacca S, Germano S, De Cecco L, et al. MicroRNA signature of malignant mesothelioma with potential diagnostic and prognostic implications. *Am J Respir Cell Mol Biol*. 2010;42(3):312-319.
16. Gee GV, Koestler DC, Christensen BC, et al. Downregulated microRNAs in the differential diagnosis of malignant pleural mesothelioma. *Int J Cancer*. 2010;127(12):2859-2869.
17. Guled M, Lahti L, Lindholm PM, et al. CDKN2A, NF2, and JUN are dysregulated among other genes by miRNAs in malignant mesothelioma—a miRNA microarray analysis. *Genes Chromosomes Cancer*. 2009;48(7):615-623.
18. Chen JF, Mandel EM, Thomson JM, et al. The role of microRNA-1 and microRNA-133 in skeletal muscle proliferation and differentiation. *Nat Genet*. 2006;38(2):228-233.
19. Yoshino H, Chiyomaru T, Enokida H, et al. The tumour-suppressive function of miR-1 and miR-133a targeting TAGLN2 in bladder cancer. *Br J Cancer*. 2011;104(5):808-818.
20. Volinia S, Galasso M, Costinean S, et al. Reprogramming of miRNA networks in cancer and leukemia. *Genome Res*. 2010;20(5):589-599.

21. Pass HI, Mew DJ. In vitro and in vivo studies of mesothelioma. *J Cell Biochem Suppl.* 1996;24:142-151.
22. Wettenhall JM, Smyth GK. limmaGUI: a graphical user interface for linear modeling of microarray data. *Bioinformatics.* 2004;20(18):3705-3706.
23. Lönnstedt I, Britton T. Hierarchical Bayes models for cDNA microarray gene expression. *Biostatistics.* 2005;6(2):279-291.
24. Benjamini Y, Hochberg Y. Controlling the false discovery rate: a practical and powerful approach to multiple testing. *J R Stat Soc Series B Stat Methodol.* 1995;57(1):289-300.
25. de Kok JB, Roelofs RW, Giesendorf BA, et al. Normalization of gene expression measurements in tumor tissues: comparison of 13 endogenous control genes. *Lab Invest.* 2005;85(1):154-159.
26. Gee HE, Buffa FM, Camps C, et al. The small-nucleolar RNAs commonly used for microRNA normalisation correlate with tumour pathology and prognosis. *Br J Cancer.* 2011;104(7):1168-1177.
27. Kassis ES, Zhao M, Hong JA, Chen GA, Nguyen DM, Schrupp DS. Depletion of DNA methyltransferase 1 and/or DNA methyltransferase 3b mediates growth arrest and apoptosis in lung and esophageal cancer and malignant pleural mesothelioma cells. *J Thorac Cardiovasc Surg.* 2006;131(2):298-306.
28. Bartel DP, Chen CZ. Micromanagers of gene expression: the potentially widespread influence of metazoan microRNAs. *Nat Rev Genet.* 2004;5(5):396-400.
29. Krützfeldt J, Rajewsky N, Braich R, et al. Silencing of microRNAs in vivo with 'antagomirs'. *Nature.* 2005;438(7068):685-689.
30. Ross DT, Scherf U, Eisen MB, et al. Systematic variation in gene expression patterns in human cancer cell lines. *Nat Genet.* 2000;24(3):227-235.
31. Yao Q, Zhang AM, Ma H, et al. Novel molecular beacons to monitor microRNAs in non-small-cell lung cancer. *Mol Cell Probes.* 2012;26(5):182-187.
32. Wang L, Shi M, Hou S, et al. MiR-483-5p suppresses the proliferation of glioma cells via directly targeting ERK1. *FEBS Lett.* 2012;586(9):1312-1317.
33. Calin GA, Dumitru CD, Shimizu M, et al. Frequent deletions and down-regulation of micro-RNA genes miR15 and miR16 at 13q14 in chronic lymphocytic leukemia. *Proc Natl Acad Sci U S A.* 2002;99(24):15524-15529.
34. Zhang L, Huang J, Yang N, et al. microRNAs exhibit high frequency genomic alterations in human cancer. *Proc Natl Acad Sci U S A.* 2006;103(24):9136-9141.
35. Datta J, Kutay H, Nasser MW, et al. Methylation mediated silencing of MicroRNA-1 gene and its role in hepatocellular carcinogenesis. *Cancer Res.* 2008;68(13):5049-5058.
36. Yan D, Dong XdaE, Chen X, et al. MicroRNA-1/206 targets c-Met and inhibits rhabdomyosarcoma development. *J Biol Chem.* 2009;284(43):29596-29604.
37. Sheikh AM, Malik M, Wen G, et al. BDNF-Akt-Bcl2 anti-apoptotic signaling pathway is compromised in the brain of autistic subjects. *J Neurosci Res.* 2010;88(12):2641-2647.
38. Sun M, Song L, Li Y, Zhou T, Jope RS. Identification of an antiapoptotic protein complex at death receptors. *Cell Death Differ.* 2008;15(12):1887-1900.
39. Niemantsverdriet M, Wagner K, Visser M, Backendorf C. Cellular functions of 14-3-3 zeta in apoptosis and cell adhesion emphasize its oncogenic character. *Oncogene.* 2008;27(9):1315-1319.
40. Pereira PM, Marques JP, Soares AR, Carreto L, Santos MA. MicroRNA expression variability in human cervical tissues. *PLoS ONE.* 2010;5(7):e11780.